VNU Journal of Science, Mathematics - Physics 26 (2010) 37-42

Effect of Cr^{3+} concentration on structural and optical properties of $ZnAl_2O_4:Cr^{3+}$

Trinh Thi Loan*, Le Hong Ha, Nguyen Ngoc Long

Faculty of Physics, Hanoi University of Science, VNU, 334 Nguyen Trai, Thanh Xuan, Hanoi

Received 10 February 2010

Abstract. $Zn(Al_{1-x}Cr_x)_2O_4$ powders with Cr^{3+} contents ranging from x = 0.005 to 0.3 have been synthesized by sol-gel method using the following precursors: zinc nitrate ($Zn(NO_3)_2 \cdot 6H_2O$), aluminium nitrate ($Al(NO_3)_3 \cdot 9H_2O$), chrome nitrate ($Cr(NO_3)_3 \cdot 9H_2O$), and citric acid. The effect of the Cr^{3+} concentration on structural and optical properties of the synthesized samples has been studied. For the samples with low Cr^{3+}-dopant concentrations, the photoluminescent (PL) spectra consist of sharp lines assigned to the $^2E(^2G) \rightarrow {}^4A_2(^4F)$ transition of ions Cr^{3+} in strong octahedral field. But for the samples with high Cr^{3+}-dopant concentrations, the PL spectra consist of a broad band centered at longer wavelengths assigned to the $^4T_2(^4F) \rightarrow {}^4A_2(^4F)$ transition of ions Cr^{3+} in weak octahedral field.

1. Introduction

The optical properties of Cr^{3+} ion located in octahedral coordination of materials such as ruby and spinel was extensively studied for several decades and these studies played an important role in the development of ligand-field theory. For the weak ligand-field, the lowest excited state is the $^4T_2(t_{2g}^2,e_g^1)$ state having the same spin multiplicity as the $^4A_2(t_{2g}^3)$ ground state, meanwhile for the strong ligand-field the lowest excited state is the $^2E(t_{2g}^3)$ state having a different spin multiplicity, but the same orbital occupancy as the $^4A_2(t_{2g}^3)$ ground state [1]. The optical properties of Cr^{3+}-doped spinel $ZnAl_2O_4$ were studied by Luc et al. [2], Wood et al. [3], Mikenda et al. [4], Nie et al. [5]. They found that the optical properties of the $ZnAl_2O_4:Cr^{3+}$ were characterized by sharp emission lines associated with the $^2E(^2G) \rightarrow {}^4A_2(^4F)$ transitions of different Cr^{3+} sites in the strong ligand-field. However, the broad luminescence band characterizing the $^4T_2(^4F) \rightarrow {}^4A_2(^4F)$ transitions of the Cr^{3+} ions in the low ligand-field has not been reported up to now.

In the present work we report the optical properties of Cr^{3+}-doped $ZnAl_2O_4$ spinel. In particular, the effect of Cr^{3+} concentration on the structural and luminescence properties of $ZnAl_2O_4:Cr^{3+}$ was investigated.

* Corresponding author. Tel: 84-4904367699.
E-mail: loan.trinhthi@gmail.com

2. Experimental

The $Zn(Al_{1-x}Cr_x)_2O_4$ powders with various Cr^{3+} contents x = 0.005, 0.01, 0.10 and 0.30 have been prepared by a sol-gel method. The powders were prepared from $Zn(NO_3)_2 \cdot 6H_2O$, $Al(NO_3)_3 \cdot 9H_2O$, $Cr(NO_3)_3 \cdot 9H_2O$, and citric acid. The aqueous solutions of $Zn(NO_3)_2 \cdot 6H_2O$, $Al(NO_3)_3 \cdot 9H_2O$ and $Cr(NO_3)_3 \cdot 9H_2O$ were mixed with the Zn^{2+} : Al^{3+} : Cr^{3+} mole ratios of 1 : 2(1-x) : 2x. Citric acid solution was added to the above solution. The final mixed solution was kept constant at a temperature of 70°C until a highly viscous gel was formed. After drying in air at 120°C for 24 h, the gel was converted to a xerogel more opaque and dense. The xerogel was annealed at a temperature of 1050°C in air for 3 h.

The crystal structure of the samples was characterized by a Siemens D5005 X-ray diffraction (XRD) diffractometer. In order to determine the elemental composition of the samples, the energy dispersive spectra (EDS) were recorded by means of an equipment JSM5410 LV & ISIS 300 JEOL Japan. PL spectra and photoluminescence excitation (PLE) spectra were measured at room temperature using a Fluorolog FL3-22 spectrofluorometer with a xenon lamp of 450 W being used as an excitation source.

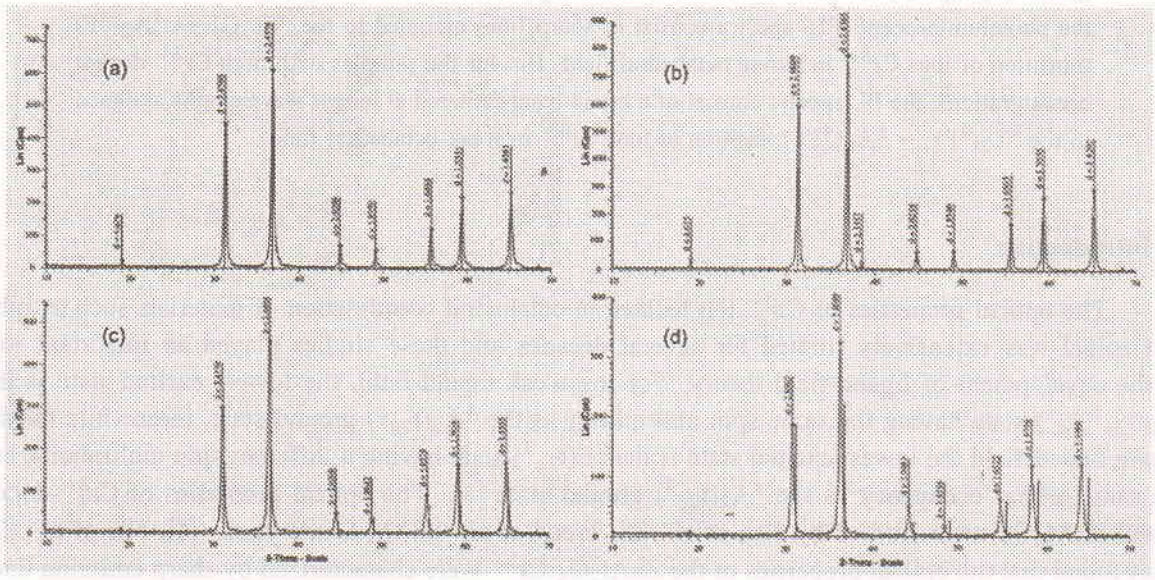

Fig. 1. The XRD patterns of the $Zn(Al_{1-x}Cr_x)_2O_4$ spinel with different mole fraction x (a) x = 0.005, (b) x = 0.01, (c) x = 0.10 and (d) x = 0.30.

3. Results and discussion

XRD analysis was performed for the $Zn(Al_{1-x}Cr_x)_2O_4$ spinel xerogel with x = 0.005 - 0.3 annealed at a temperature of 1050°C for 4 h. In figure 1 XRD patterns of the spinel xerogel doped with x = 0.005, 0.01, 0.10 and 0.30 are represented. As evident from the figure, the samples are single-phase material with good crystallinity and all the peaks can be assigned to the spinel $ZnAl_2O_4$ phase. No characteristic peaks of impurity phase have been observed. It can be noticed that with increasing the mole fraction x, the position of the diffraction peaks shifted towards the small-theta

Table 1. The dependence of d_{hkl} and lattice constants on the mole fraction x of the $Zn(Al_{1-x}Cr_x)_2O_4$.

x	d_{220}(nm)	d_{311}(nm)	d_{422}(nm)	d_{511}(nm)	d_{440}(nm)	a(nm)
0.005	0.2859	0.2438	0.1648	0.1555	0.1428	0.8081±0.0003
0.01	0.2861	0.2439	0.1650	0.1556	0.1429	0.8086±0.0003
0.10	0.2875	0.2449	0.1657	0.1562	0.1436	0.8122±0.0005
0.30	0.2896	0.2470	0.1672	0.1576	0.1446	0.8189±0.0004

side, which is associated with an increase in the d_{hkl} and the lattice constants. With increasing the lattice constants the Zn^{2+} - O^{2-}, Al^{3+} - O^{2-}, Cr^{3+} - O^{2-} distances increase. The result is that the ligand-field influenced Cr^{3+} ion is decreased. The values of d_{hkl} and lattice constants of the samples calculated from the XRD patterns are shown in table 1.

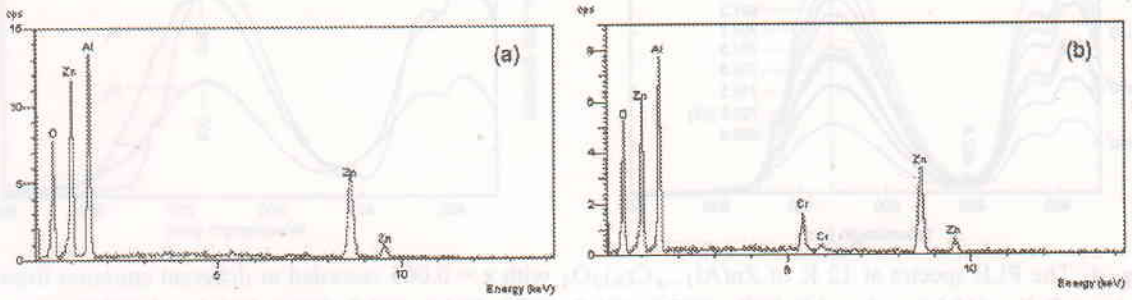

Fig. 2. The energy dispersive spectra of the $Zn(Al_{1-x}Cr_x)_2O_4$ spinel with different mole fraction x. (a) x = 0.005 and (b) x = 0.10.

Figure 2 shows the EDS of the $Zn(Al_{1-x}Cr_x)_2O_4$ spinel with x = 0.005 and 0.10, in which some characteristic X-ray peaks originating from Zn, Al, O and Cr are observed. However, Cr element is only detected with sample x = 0.10. In sample x = 0.005, Cr element is not detected due to a relatively low dopant concentration.

Figure 3 shows the PL spectra of the $Zn(Al_{1-x}Cr_x)_2O_4$ with x = 0.005 at 12 and 300 K excited by 390 nm wavelength. In the spectrum at 12 K is observed a very distinct zero-phonon R-line

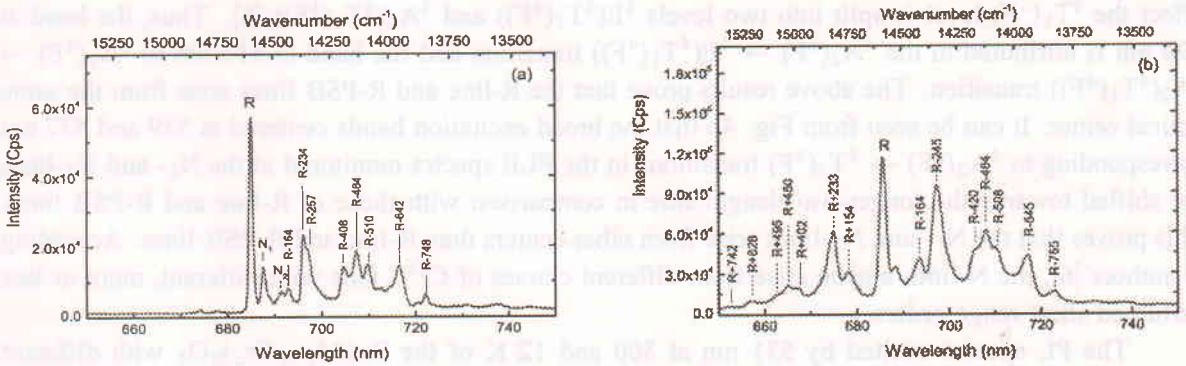

Fig. 3. The PL spectra excited by 390 nm wavelength of the $Zn(Al_{1-x}Cr_x)_2O_4$ with x = 0.005 at different temperatures. (a) 12 K and (b) 300 K. The phonon-sideband of R-line is denoted by R±250, where 250 is energy (in cm^{-1}) of the phonon, the sign (-) corresponds to the emission of phonon, the sign (+) to the absorption of phonon.

at 685.5 nm corresponding to the $^2E(^2G) \rightarrow {}^4A_2(^4F)$ transition. In addition, there are found many phonon-sidebands (PSBs) of R-line (Stokes' lines) as shown in figure 3(a). Whereas in the spectrum at 300 K depicted in figure 3(b) on the shorter-wavelength side of R-line appear many anti-Stokes' lines originated from the $^2E(^2G) \rightarrow {}^4A_2(^4F)$ transitions accompanying an absorption of the phonons. From figure 3 it is noticed that the two emission lines N_1 (687.6 nm) and N_2 (691.3 nm) do not relate to the R-line and the phonon-sidebands of the R-line (R-PSB) because the corresponding anti-Stokes' lines are absent in the spectrum at room temperature. Therefore, the N_1- and N_2-lines must arise from other emission centers than the R-line and R-PSB.

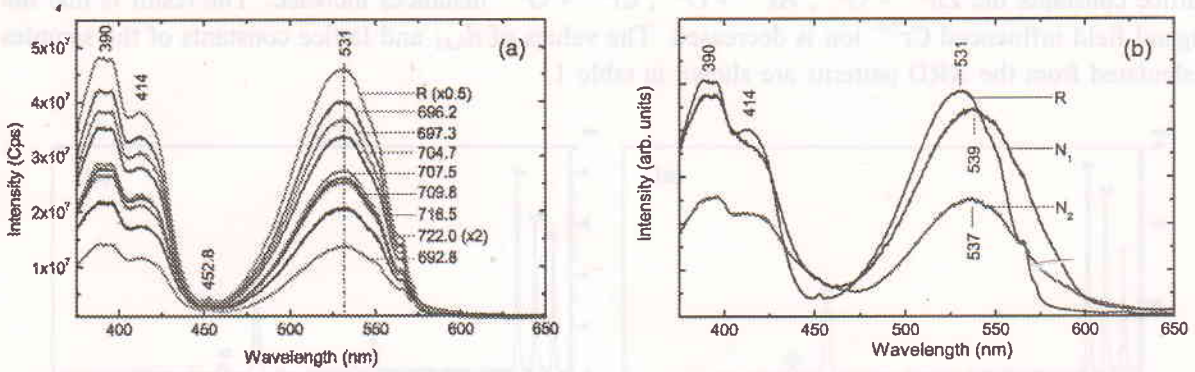

Fig. 4. The PLE spectra at 12 K of $Zn(Al_{1-x}Cr_x)_2O_4$ with x = 0.005 recorded at different emission lines: (a) at R-line (685.5 nm) and R-PSBs (692.8, 696.2, 697.3, 704.7, 707.5, 709.8, 716.5 and 722.0 nm); (b) at the R-line and the N_1-, N_2-lines.

In order to confirm the above-mentioned interpretation, the measurements of PLE spectra were performed. The results showed that the PLE spectra monitored at the R-PSBs: R-164 (692.8 nm), R-234 (696.2 nm), R-257 (697.3 nm), R-408 (704.7 nm), R-464 (707.5 nm), R-510 (709.8 nm), R-642 (716.5 nm) and R-748 (722.0 nm) are similar to those recorded at R-line at 685.5 nm (figure 4(a)). The PLE spectra consisted of two strong broad bands. The broad band centered at 531 nm corresponds to $^4A_2(^4F) \rightarrow {}^4T_2(^4F)$ transitions, meanwhile two bands centered at 390 and 414 nm correspond to $^4A_2(^4F) \rightarrow {}^4T_1(^4F)$ transitions. It is noticed that in the trigonal crystal field and under the spin-orbit effect the $^4T_1(^4F)$ level is split into two levels $^4E(^4T_1(^4F))$ and $^4A_2(^4T_1(^4F))$ [5]. Thus, the band at 390 nm is attributed to the $^4A_2(^4F) \rightarrow {}^4E(^4T_1(^4F))$ transition and the band at 414 nm to $^4A_2(^4F) \rightarrow {}^4A_2(^4T_1(^4F))$ transition. The above results prove that the R-line and R-PSB lines arise from the same optical center. It can be seen from Fig. 4b that the broad excitation bands centered at 539 and 537 nm corresponding to $^4A_2(^4F) \rightarrow {}^4T_2(^4F)$ transitions in the PLE spectra monitored at the N_1- and N_2-lines are shifted towards the longer-wavelength side in comparison with those of R-line and R-PSB lines. This proves that the N_1- and N_2-lines arise from other centers than R-line and R-PSB lines. According to authors [6], the N-lines maybe arise from different classes of Cr^{3+} ions with different, more or less perturbed short range orders.

The PL spectra excited by 531 nm at 300 and 12 K of the $Zn(Al_{1-x}Cr_x)_2O_4$ with different mole fraction x are presented figure 5. The results showed that the intensity ratio of the 706.0, 722.8, 740.0, 745.7 and 754.0 nm lines to 685.5 nm line at 300 K (figure 5(a)) increases with increasing mole fraction x in ranging from x = 0.005 to 0.04. The increase of the intensity ratio of the 704.5, 727, 730, 737, 745 and 754 nm lines to 685 nm line with increasing mole fraction x was more clearly observed

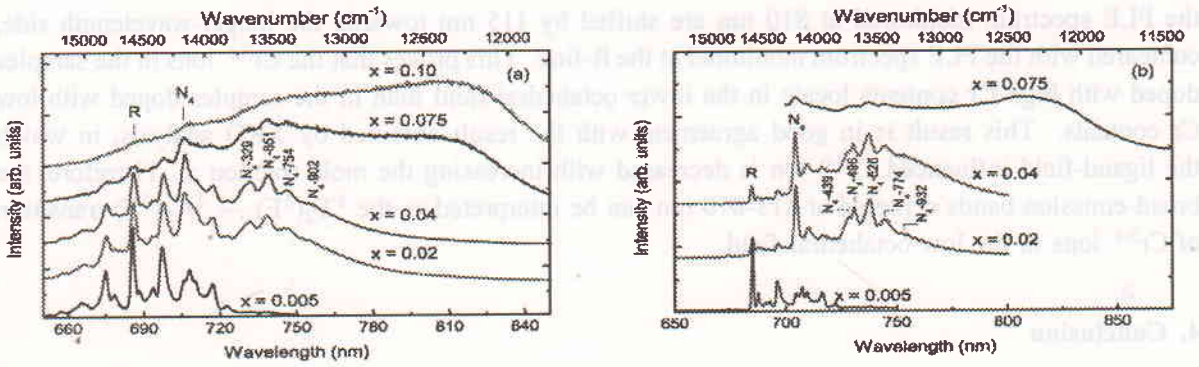

Fig. 5. The PL spectra excited by 531 nm at (a) 300 K and (b) 12 K of the $Zn(Al_{1-x}Cr_x)_2O_4$ with different mole fraction x.

at 12 K (figure 5(b)). In order to find out about the origin of the emission lines, PLE spectra at 12 K were measured. It can be seen from figure 6(a), the PLE spectra monitered at emission wavelengths 727, 730, 737, 745 and 754 nm lines are similar to that recorded at 704.5 nm line. It is well known that in the samples with the enough high Cr^{3+}-concentrations, the Cr^{3+} ions have the possibility of pairing. Therefore, like the previous reports [2, 4, 5], the 704.5 nm line (denoted by N_4) in the PL spectrum measured at 12 K is interpreted to arise from Cr^{3+} - Cr^{3+} pairs and 727, 730, 737, 745 and 754 nm lines are the phonon-sidebands of N_4-line: N_4-439 (727 nm), N_4-496 (730 nm), N_4-626 (737 nm), N_4-774 (745 nm) and N_4-932 (754 nm).

In particular, as increasing mole fraction x up to 0.075 and more, on the long wavelength side of the N_4-lines a very broad emission band centered at 813 nm at 300 K (figure 5(a)) or at 810 nm at 12 K (figure 5(b)) appeared. In the PL spectrum of the sample $Zn(Al_{1-x}Cr_x)_2O_4$ with x = 0.10 the short-wavelength lines are extremely weak, and the spectrum is dominated by the broad emission band centered at 813 nm.

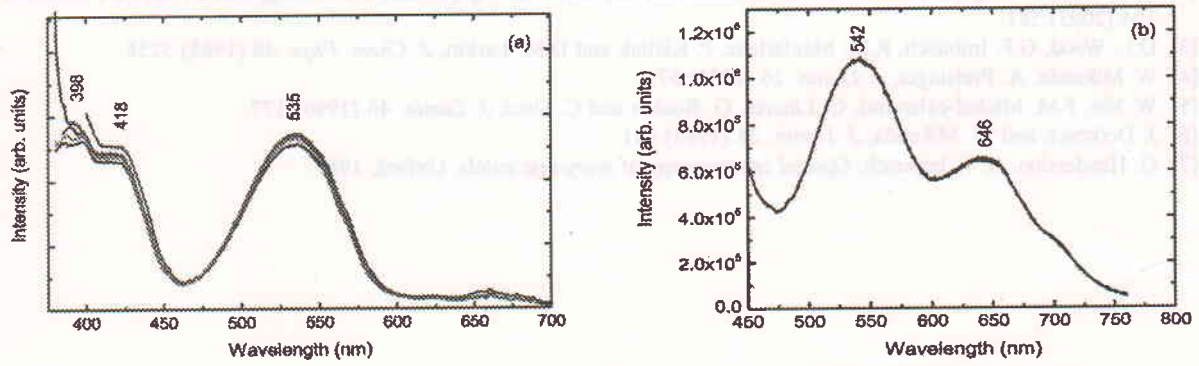

Fig. 6. The PLE spectra at 12 K of the $Zn(Al_{1-x}Cr_x)_2O_4$ with x = 0.075 monitored at different emission wavelength: (a) N4-439 (727 nm), N4-496 (730 nm), N4-626 (737 nm), N4-774 (745 nm) and N4-932 (754 nm); (b) 810 nm.

Figure 6(b) shows the PLE spectrum at 12 K of the $Zn(Al_{1-x}Cr_x)_2O_4$ with x = 0.075 recorded at 810 nm. Two broad excitation bands are detected. The band at 542 nm corresponds to $^4A_2(^4F) \rightarrow {}^4T_1(^4F)$ transitions and the band at 646 nm to $^4A_2(^4F) \rightarrow {}^4T_2(^4F)$ transitions [7]. It is seen from figure 6(b) and figure 4(b) that the broad excitation band corresponding to $^4A_2(^4F) \rightarrow {}^4T_2(^4F)$ transition in

the PLE spectrum monitored at 810 nm are shifted by 115 nm towards the longer-wavelength side, compared with the PLE spectrum monitored at the R-line. This proves that the Cr^{3+} ions in the samples doped with high Cr contents locate in the lower octahedral field than in the samples doped with low Cr contents. This result is in good agreement with the result obtained by XRD analysis, in which the ligand-field influenced Cr^{3+} ion is decreased with increasing the mole fraction x. Therefore, the broad emission bands centered at 813-810 nm can be interpreted as the $^4T_2(^4F) \rightarrow {}^4A_2(^4F)$ transition of Cr^{3+} ions in the low octahedral field.

4. Conclusion

The effect of Cr^{3+} dopant concentration on the structural and optical properties of the synthesized samples $Zn(Al_{1-x}Cr_x)_2O_4$ has been studied. With increasing Cr contents, the lattice constants increase and the ligand-field surrounding Cr^{3+} ions is decreased. For the samples with low Cr^{3+} dopant concentrations, the PL spectra mainly consist of sharp lines (R-line and R-PSB) assigned to the $^2E(^2G) \rightarrow {}^4A_2(^4F)$ transitions of ions Cr^{3+} in strong octahedral field. With increasing Cr^{3+} contents the PL spectra exhibit the PL lines (N_4-line and N_4-PSB) related to the transitions in the Cr^{3+} - Cr^{3+} pairs. Further increasing Cr^{3+} dopant concentrations up to an appropriate value, in the PL spectra a broad band centered at 810-813 nm appears. This broad band is assigned to the $^4T_2(^4F) \rightarrow {}^4A_2(^4F)$ transition of ions Cr^{3+} in weak octahedral field.

Acknowledgments. This work is financially supported by Ministry of Science and Technology of Vietnam (Project No 103.02.51.09 from NAFOSTED).

References

[1] M. Milos, S. Kairouani, S. Rabaste, A. Hauser, *Coordination chemistry Reviews* 252 (2008) 2540.
[2] H.H. Luc, T.K. Nguyen, A. Suchocki, A. Kaminska, V.K. Le, V.H. Nguyen and T.T. Luong, *ACTA Physica Polinica* A 104 (2003) 581.
[3] D.L. Wood, G.F. Imbusch, R.M. Macfarlane, P. Kisliuk and D.M. Larkin, *J. Chem. Phys.* 48 (1968) 5255.
[4] W. Mikenda, A. Preisinger, *J. Lumin.* 26 (1981) 67.
[5] W. Nie, F.M. Michel-calendini, C. Linares, G. Boulon and C. Daul, *J. Lumin.* 46 (1990) 177.
[6] J. Derkosch and W. Mikenda, *J. Lumin.* 28 (1983) 431.
[7] G. Hendersion, G. F. Imbusch, *Optical spectroscopy of inorganic solids*, Oxford, 1989.